

Pushing the Limits of Sparsity: A Bag of Tricks for Extreme Pruning

Andy Li^{1,†}, Aiden Durrant¹, Milan Markovic¹, Lu Yin² and Georgios Leontidis¹
¹ University of Aberdeen (UK), ²University of Surrey (UK)

[†]corresponding author: a.li.21@abdn.ac.uk

Abstract

*Pruning of deep neural networks has been an effective technique for reducing model size while preserving most of the performance of dense networks, crucial for deploying models on memory and power-constrained devices. While recent sparse learning methods have shown promising performance up to moderate sparsity levels such as 95% and 98%, accuracy quickly deteriorates when pushing sparsities to extreme levels. Obtaining sparse networks at such extreme sparsity levels presents unique challenges, such as fragile gradient flow and heightened risk of layer collapse. In this work, we explore network performance beyond the commonly studied sparsities, and propose a collection of techniques that enable the continuous learning of networks without accuracy collapse even at extreme sparsities, including 99.90%, 99.95% and 99.99% on ResNet architectures. Our approach combines 1) Dynamic ReLU phasing, where DyReLU initially allows for richer parameter exploration before being gradually replaced by standard ReLU, 2) weight sharing which reuses parameters within a residual layer while maintaining the same number of learnable parameters, and 3) cyclic sparsity, where both sparsity levels and sparsity patterns evolve dynamically throughout training to better encourage parameter exploration. We evaluate our method, which we term **Extreme Adaptive Sparse Training (EAST)** at extreme sparsities using ResNet-34 and ResNet-50 on CIFAR-10, CIFAR-100, and ImageNet, achieving significant performance improvements over state-of-the-art methods we compared with.*

1. Introduction

Network pruning [9, 10, 15, 16, 19, 22] is a widely-used technique for reducing a network’s parameters and compressing its size. Reducing model sizes is crucial for deploying models on edge devices with limited resources. Conventionally, pruning methods have focused on reducing parameters from pre-trained models. However, it requires at least as much computation as training a dense model as it must converge before pruning takes place. The Lot-

tery Ticket Hypothesis [6, 7, 23] has shown that there exist subnetworks that can perform as well as the dense counterpart, even when trained from an initially sparse state. This insight has recently gained much traction in sparse training, a paradigm in which sparse networks are trained from scratch without the need for dense pre-training, promising efficiency gains in both memory and computation.

Sparse training methods can be broadly classified into two categories: static sparse training (SST), also sometimes referred to as Pruning at Initialization (PAI), where the sparsity pattern is pre-determined at initialization and remains fixed throughout training [2, 17, 30, 33], and dynamic sparse training (DST), where the sparsity pattern continuously evolves during training [3, 4, 25, 34]. They have shown promising results at retaining most of the performance at moderate sparsity levels, commonly up to 98% in recent literature. However, most of these begin experiencing rapid degradation in accuracy beyond these levels due to limitations such as layer collapse and rapid gradient degradation [31, 33]. While the focus has largely been on preserving performance at moderate sparsities, there is an increasing demand to push towards ‘extreme sparsities’, where achieving substantial model compression at the cost of performance trade-offs may be necessary. This shift is particularly crucial in resource-constrained settings, where aggressive sparsification can have substantial computational and memory benefits, even if some accuracy must be sacrificed. Despite this need, extreme sparsities remain relatively understudied, with only a few methods attempting to maintain usable accuracy at these extreme levels [2, 28, 31].

Our work proposes a collection of adaptive methods that when combined can achieve meaningful performance at extreme sparsities. By leveraging three core strategies - 1) phased Dynamic ReLU activation, 2) weight sharing, 3) cyclic sparsity scheduling - we present a flexible framework that is capable of optimizing performance at extreme sparsities. Each component independently enhances the sparse model’s capacity as seen in our ablation studies, where individual strategy improves performance on their own. However, when used together, these methods can cohesively achieve an even stronger performance. This framework,

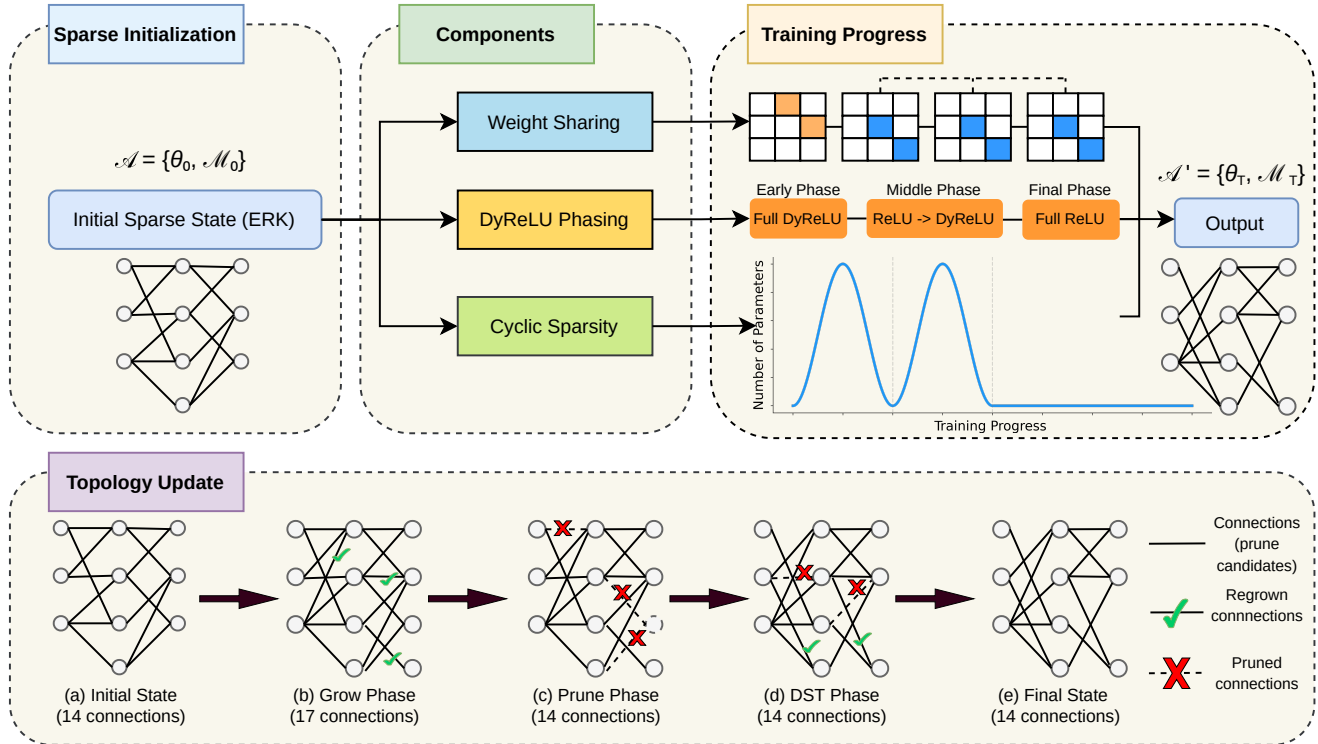


Figure 1. Illustration of EAST (top). Starting with ERK-initialized sparse network $\mathcal{A} = \{\theta_0, \mathcal{M}_0\}$ at sparsity s , EAST employs three key components: DyReLU phasing, weight sharing, and cyclic sparsity to transform the network to final state $\mathcal{A}' = \{\theta_T, \mathcal{M}_T\}$, achieving meaningful performance at extreme sparsity levels. The topology update box (bottom) illustrates the connectivity change throughout training: connections are first grown, then pruned, and eventually maintained with a fixed sparsity update schedule until completion.

which we term **Extreme Adaptive Sparse Training (EAST)**, offers a modular approach that can be adapted to existing DST frameworks, effectively postponing their total performance collapse, as shown in Figure 2. Through empirical analysis, we find that EAST prevents gradient vanishing and encourages parameter exploration, achieving substantial and meaningful performance gain over our baselines. Our contribution and key achievements can be summarized as follows:

- We introduce EAST - a method that combines phased Dynamic ReLU activation, weight sharing, and cyclic sparsity scheduling, aimed at retaining performance past common sparsity thresholds.
- We perform extensive empirical evaluation of EAST on computer vision tasks, and demonstrate that it can achieve superior performance at sparsities beyond 99.90%, surpassing all previous methods tested.
- We explore and demonstrate that DyReLU when used as a drop-in replacement for ReLU at initialization at then replaced completely can still improve the parameter exploration at extreme sparsities, leading to higher performance than sparse models trained using ReLU only.

- To the best of our knowledge, EAST is the first DST method to dynamically adjust both sparsity patterns and sparsity levels throughout training (as opposed to just the patterns). Our cyclic sparsity schedule allows models to explore parameters and stabilize at extreme sparsity, as evidenced by our ablation studies.
- Unlike DCTpS, EAST achieves extreme sparsity without requiring dense matrix computations for inference, resulting in a truly lightweight and efficient model for edge deployment. We also demonstrate the versatility of our method by combining with DCT layers on top of DST, consistently improving accuracy at the tested settings.

2. Related Work

2.1. Dynamic Sparse Training

Early work by Mocanu et al. demonstrated the viability of DST through SET [25], which used magnitude pruning and random weight regrowth. Subsequent criteria for regrowing connections have been developed, such as using the momentum of parameters in SNFS [3] or their gradient in RigL [4] to determine the saliency of deactivated connections. GraNet [20] adapted RigL’s approach by starting

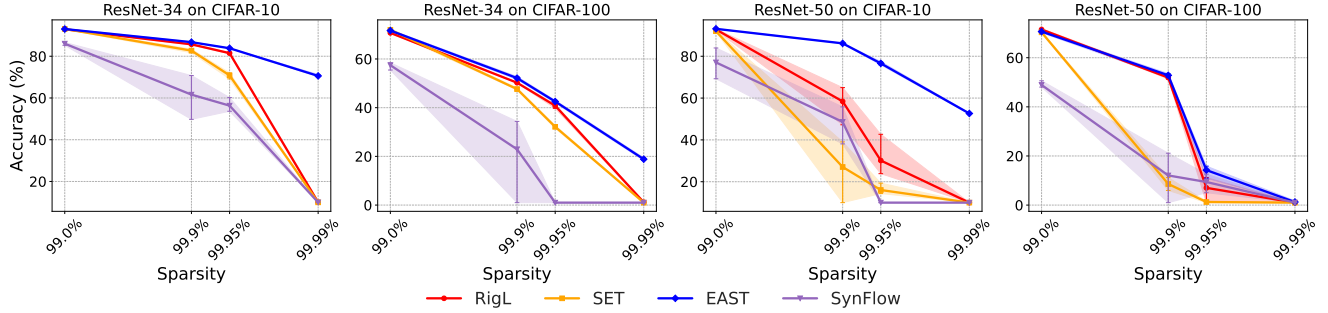


Figure 2. Comparison of test accuracies across different sparsities. Each point represents median accuracy over three runs with different seeds, and the shaded regions highlight the variability across runs.

with half the parameters and gradually increasing to target sparsity instead of starting from the target sparsity. ITOP [21] provides a deeper understanding of pre-existing DST methods and enhances parameter exploration during sparse training. NeurRev [18] addressed the issue of dormant neurons by removing harmful negative weights. Recent advances include Top-KAST [13], which maintains an auxiliary set of weights for enhanced exploration, and BiDST [14] which formulates DST as a bi-level optimization problem for joint weight-mask optimization. MEST [36] introduces a memory-efficient sparse training framework for edge devices, while Chase [35] adapts dynamic unstructured sparsity into hardware-friendly channel-wise sparsity, both optimizing performance on resource-constrained systems without sacrificing accuracy. BiDST [14] formulates DST as a bi-level optimization problem, where both weights and masks are optimized simultaneously resulting in higher mask exploration efficiency. Supticket [34] further enhances the performance of DST by leveraging weight averaging at the late training stage.

2.2. Extreme Sparsity Methods

Most current methods focus on sparsity levels at which pruned networks can match or closely approximate the performance of their dense counterparts [8]. However, there is growing interest in extreme sparsities, where accuracy trade-offs become inevitable but potentially worthwhile for substantial computational gains. Yet there remains challenges, such as maintaining stable gradient flow and preventing layer collapse, which conventional pruning methods struggle to address. GraSP [33] and SynFlow [31] specifically addressed the gradient preservation and layer collapse issues at high sparsities via careful network initialization. SNIP [17] and SNIP-it [32] proposed PaI methods that showed promising results at higher sparsities, though primarily focused on static masks. De Jorge et al. [2] demonstrated that methods like SNIP and GraSP can perform worse than random pruning at 99% sparsity and beyond, and proposed iterative pruning approaches (Iter-SNIP

and FORCE) that maintained meaningful performance up to 99.5% sparsity through gradual parameter elimination. DCTpS [28] introduced "DCT plus Sparse" layers that combined a fixed dense DCT offset matrix with trainable sparse parameters to maintain propagation at extreme sparsities up to 99.99%.

2.3. Activation Functions

Activation functions in sparse networks have traditionally relied on static activation functions such as ReLU [27], which applies a fixed threshold to the input. Parametric variants such as PReLU [11] introduced learnable parameters to adapt the negative slope, offering slight improvements in gradient flow. Swish [29] and Mish [24] aim to smooth gradients for better optimization but remain static throughout training. Dynamic ReLU (DyReLU) [1] introduced an adaptive activation that dynamically adjusts the slopes of a ReLU based on the input.

3. Methodology

3.1. Activation Function

In this work, when initializing a network, we replace the standard ReLU activation with Dynamic ReLU (DyReLU), specifically the DyReLU-B variant, which dynamically adapts and adjusts channel-wise activation coefficients during training, allowing the model to explore a larger space of activation functions. Preliminary details about DyReLU and DST related to this section can be found in Supplementary Material. At extreme sparsities (e.g., > 99%), networks rapidly start losing expressive power. DyReLU compensates for this by dynamically adjusting the activation functions to adapt to the reduced network capacity. By using this during the early stages of training, we allow the network to explore a larger activation space and prevent premature collapse due to over-pruning.

We hypothesize that DyReLU can help networks better explore and optimize parameters at extreme sparsities by dynamically adjusting the activations during the critical

early phases of training. This allows the network to better handle the challenges introduced by the sparse structure (e.g., loss of representational capacity), as the dynamic activations can help identify and amplify important features in the sparse subnetwork. We detail the ablation studies on the effect of DyReLU in section 4.3.

Phasing out DyReLU: As training progresses, we phase out all DyReLU and gradually replace them with the standard ReLU. We introduce a hyperparameter that regulates the contribution of DyReLU during training. It makes full contribution when it is 1, and gradually decreases to 0 as training progresses, eventually reaching 0 before the first learning rate decay, at which point DyReLU has been completely replaced by ReLU. We find that this helps the network settle into a more stable configuration, as DyReLU is no longer needed once the network has explored the parameter space adequately. This process removes all DyReLU-introduced parameters.

The *decay factor* for this transition is denoted as $\beta(t)$, which decays linearly over the course of training:

$$\beta(t) = 1 - \frac{t - t_{\text{start}}}{t_{\text{end}} - t_{\text{start}}}$$

where t_{start} and t_{end} denote the start and end epochs of DyReLU phasing. We choose t_{end} to be the epoch before the first learning rate schedule update in all of our runs. We initialize with:

$$f(x; t = 0) = f_{\text{DyReLU}}(x)$$

During the transition, the activation function progressively shifts toward ReLU:

$$f(x; t) = \beta(t) \cdot f_{\text{DyReLU}}(x) + (1 - \beta(t)) \cdot f_{\text{ReLU}}(x)$$

By the end of phasing $t = T_{\text{end}}$, we have:

$$f(x; t = T_{\text{end}}) = f_{\text{ReLU}}(x)$$

This smooth transition from a dynamic to static activation function prevents the network from overfitting to a complex activation pattern while still reaping the benefits of DyReLU in the early stages of training.

Theorem: During DyReLU to ReLU transition with decay factor $\beta(t)$, the gradient flow is strictly greater than standard ReLU such that:

$$\|\nabla \mathcal{L}\|_{\text{DyReLU} \rightarrow \text{ReLU}} > \|\nabla \mathcal{L}\|_{\text{ReLU}} \quad \text{for } \beta(t) \geq 0$$

The proof for this can be found in Supplementary Materials. In the experiments, we show how this method initially boosts the gradient flow, and then keeps it even after β reaches zero.

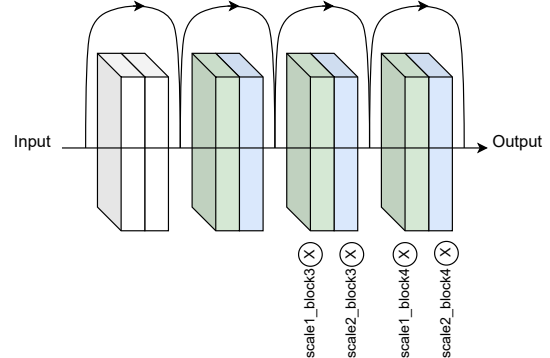


Figure 3. A layer in ResNet-34 with 4 blocks. Block 3 and Block 4 share parameters (and the masks) with block 2. Specifically, conv1 layer (green) of block 3 reuses conv1 layer of block 2, and is multiplied by a learnable scaling factor; similarly, its conv2 layer (blue) reuses conv2 layer of block 2, and is multiplied by another scaling factor.

3.2. Weight Sharing

Much research in sparse training has been about path optimization - that is obtaining the right mask, or the right set of learnable parameters that are most important to the outcome. We ask the question: *Can increasing the number of paths for gradient propagation while maintaining number of learnable parameters help maintain stable training at extreme sparsities?* We hypothesize that creating more paths for gradient propagation through shared parameters can strengthen gradient flow, and lead to stronger overall gradient flow.

To test our hypothesis, we introduce a weight sharing mechanism across residual blocks within each layer that preserves gradient flow without increasing the overall count of learnable parameters. Specifically, we choose a block inside a layer and share its parameters (along with their masks) with all blocks after it. These blocks reference the single block tensor that they share with, and multiply by a scaling factor for forward and backward passes. They do not need to be physically stored multiple times in memory, making the approach memory-efficient. Thus, we adjust sparsity calculation to reflect this architectural modification, such that sparsity $s = 1 - \frac{\|\mathcal{M} \odot \theta_{\text{learnable}}\|_0}{\|\theta\|_0}$, where $\|\cdot\|$ is the ℓ_0 -norm or the cardinality, $\theta_{\text{learnable}}$ is the learnable parameters, and θ is the theoretical parameters in the original network with a mask $\mathcal{M} \in \{0, 1\}^{|\theta|}$. In our experiments, we share the second block with the rest of the blocks within a layer. For instance, as shown in Figure 3, if a layer has 4 blocks, the second block shares its parameters and sparse topology with the 3rd and 4th block.

Formally, let L be the number of residual blocks in a layer, and R be the block that shares parameters ($1 < R \leq$

L), where the remaining $L-R$ blocks share parameters with the R -th block. Let θ_i represent the parameters of the i -th block. Our weight sharing scheme can be expressed as:

$$\theta_i = \begin{cases} \theta_i & \text{if } i \leq R \\ \theta_R & \text{if } R < i \leq L \end{cases}$$

3.3. Cyclic Sparsity

While standard DST methods such as SET and RigL adjust the sparsity pattern, sparsity s is consistent throughout training - pruning and regrowing of weights take place at the same t . i.e., $\mathcal{M}(t) = \text{Prune}(\theta(t)) \cup \text{Grow}(\nabla_{\theta}\mathcal{L})$.

Algorithm 1 Pseudocode for EAST

Input: Sparse neural network with weights θ , maximum sparsity s_{\max} , minimum sparsity s_{\min} , end of cyclic sparsity T_c , update frequency ΔT , prune rate r_p , DyReLU phase start T_s , end T_e

Output: Trained θ_s

```

1: Initialize:  $\theta_s$  at  $s_{\max}$ ,  $\phi \leftarrow \text{DyReLU}$ 
2: for  $t = 1$  to  $T_{\text{end}}$  do
3:   for  $T_s \leq t \leq T_e$  do ▷ DyReLU to ReLU
4:      $\phi \leftarrow \beta \text{DyReLU} + (1 - \beta) \text{ReLU}$ 
5:     Update( $\beta$ )
6:   end for
7:   if  $t \bmod \Delta T == 0$  then
8:     if  $t \leq T_c$  then
9:        $s_{\text{target}} \leftarrow s_{\min} + \frac{s_{\max} - s_{\min}}{2} \cdot (1 + \cos(2\pi t/T_c))$ 
▷ Update target sparsity
10:      if  $s_{\text{target}} > s_{\text{current}}$  then
11:         $\theta_s \leftarrow \theta_s - \text{ArgTopK}(-|\theta_s|, (s_{\text{target}} - s_{\text{current}})\|\theta_s\|_0)$ 
▷ Magnitude pruning
12:      else if  $s_{\text{target}} < s_{\text{current}}$  then
13:         $\theta_s \leftarrow \theta_s + \text{ArgTopK}(|\nabla_{\theta}\mathcal{L}|, (s_{\text{current}} - s_{\text{target}})\|\theta_s\|_0)$ 
▷ Gradient regrowth
14:      end if
15:    else ▷ Switch to fixed update
16:       $\theta_s \leftarrow \theta_s - \text{ArgTopK}(-|\theta_s|, r_p\|\theta_s\|_0)$ 
17:       $\theta_s \leftarrow \theta_s + \text{ArgTopK}(|\nabla_{\theta}\mathcal{L}|, r_p\|\theta_s\|_0)$ 
18:    end if
19:  end if
20: end for
21: return  $\theta_s$ 

```

In our work, we introduce a cyclic sparsity schedule where the network’s sparsity level itself evolves dynamically during training. Instead of maintaining a constant sparsity, we cyclically adjust the sparsity $s(t)$ between a maximum value s_{\max} and a minimum value s_{\min} . The sparsity level $s(t)$ is governed by a cosine schedule:

$$s(t) = s_{\min} + \frac{s_{\max} - s_{\min}}{2} \cdot \left(1 + \cos\left(\frac{2\pi t}{T_c}\right)\right)$$

where T_c is the period of the cyclic sparsity. This schedule ensures that the sparsity grows smoothly to s_{\max} and then gradually reduces to s_{\min} . As a result, the network experiences phases of higher and lower connectivity, promoting better parameter exploration during training. Once the cyclic phase ends at T_c , we fix the sparsity and switch to a static pruning and growth update. The details of our method are summarized in Algorithm 1.

4. Experiments

Our experiments include image classification using ResNet34 and ResNet50 [12] on computer vision datasets CIFAR-10 and CIFAR-100, and ResNet50 on ImageNet. We compare our method with DST methods SET[25] and RigL[4], and a competitive SST method SynFlow[31], which also experiments at very high sparsity. We collectively refer to these methods as sparse training methods for the rest of the paper. For SynFlow, we use the official repository with its default hyperparameters to evaluate its performance. For SET and RigL, we use the repository provided by ITOP [21]. We keep all hyperparameters as they are optimally configured in the paper, including ΔT , ERK initialization, the mask update interval of 1500 and 4000 for SET and RigL, respectively.

In addition, we benchmark DCT, the SOTA method specifically focused on extreme sparsity using the repository provided by the paper [28]. While this method performs very competitively at extreme sparsity settings, it comes at a cost due to the computation of a dense matrix matching the full architecture size, which adds an extra layer of computational overhead and requires extra memory. This method achieves the best performance when paired with RigL, which we evaluate, and then we combine it with our approach to evaluate if our method can improve it further. In this integration, we use only DyReLU phasing and cyclic density, leaving weight sharing to prevent conflicts with the DCT matrices embedded in the model architecture. Here, we use $\Delta T = 100$ to match results from the original paper, and we also use this value for our integration to ensure fairness.

For all DST methods, we use SGD with momentum as our optimizer. The momentum coefficient is set to 0.9, and L2 regularization coefficient is set to 0.0001. We set the training epoch to 250 and use a learning rate scheduler that decreases from 0.1 by a factor of 10X at half way and three-quarters of way through training. For the DCT experiments, we train for 200 epochs with the Adam optimizer and a learning rate of 0.001. A more detailed description of the experimental setups and hyperparameters is included in the Supplementary Material. All experiments in our work are conducted on an A100 GPU.

Method	CIFAR-10				CIFAR-100			
	99%	99.90%	99.95%	99.99%	99%	99.90%	99.95%	99.99%
ResNet-34								
Synflow	82.03	61.61	56.33	10.00	57.44	22.91	1.00	1.00
SET	93.09	82.70	70.84	10.00	71.97	47.64	32.14	1.00
RigL	92.92	85.71	81.47	10.03	71.72	50.26	40.92	1.14
EAST (<i>ours</i>)	93.03	86.76	83.83	70.57	72.01	52.16	42.53	18.84
DCTpS+RigL	89.04	83.96	80.80	77.38	63.12	51.30	45.68	37.59
DCTpS+RigL+EAST (<i>ours</i>)	89.22	84.19	81.96	77.54	64.33	53.21	47.80	38.02
ResNet-50								
Synflow	77.06	48.62	10.00	10.00	48.91	12.07	9.40	1.00
SET	91.97	27.05	16.04	10.00	70.35	8.59	1.26	1.00
RigL	92.75	58.41	30.14	10.00	70.50	51.93	7.02	1.00
EAST (<i>ours</i>)	93.12	86.16	76.60	54.63	70.64	52.84	14.23	1.88
DCTpS+RigL	89.66	85.98	85.03	83.13	64.85	55.98	52.71	49.63
DCTpS+RigL+EAST (<i>ours</i>)	89.67	87.10	85.87	83.88	64.92	58.17	55.60	51.33

Table 1. Accuracy comparison on CIFAR-10 and CIFAR-100 at different sparsity levels. Top section compares sparse training methods at each sparsity level. Bottom section shows results with DCTpS, which achieves higher accuracies at $\geq 99.95\%$ sparsity, but requires dense matrix computations. The best results for each category are in bold.

4.1. CIFAR-10 and CIFAR-100

We evaluate EAST on CIFAR-10 and CIFAR-100 classification tasks using ResNet34 and ResNet50, with a particular focus on extreme sparsities (99%-99.99%). We repeat our experiments three times and report the average accuracy in Table 1, which includes the comprehensive results across different configurations.

At 99%, all dynamic training methods achieve comparable performance, significantly outperforming SynFlow. This is unsurprising as a static mask is expected to lead to worse performance than a dynamic mask [4, 26]. EAST’s advantages become increasingly pronounced at higher sparsities. At 99.90% and 99.95%, EAST beats the next best performing method RigL by a clear margin ranging between 1-2% with ResNet34 on both datasets, showing significant gains in performance. The difference becomes even more clear with ResNet50, where other methods take a huge plummet on accuracy and EAST shows a more gradual decline. EAST displays an improvement of 38-40% over RigL on CIFAR-10, and 1-7% on CIFAR-100 at 99.90% and 99.95%.

The most striking difference appears at 99.99%. We observe that all other methods result in complete collapse to random performance on either dataset and model. In contrast, EAST maintains meaningful accuracies with the exception of ResNet50 on CIFAR-100. For instance, EAST achieves 70.57% on CIFAR-10 compared to 10% random baselines. This pattern holds across both models, though ResNet50 shows more degradation at the highest sparsity

levels, presumably due to more prominent vanishing gradient problems in a deeper network, with even fewer parameters spread across each layer.

We evaluate DCT and find that while DCT performs significantly better at 99.95% and 99.99%, it performs worse than SET, RigL and EAST at 99% and sometimes 99.9%. For instance, EAST achieves 3-8% higher accuracy than DCT at 99%, without involving the additional overhead. We further combine DCT and EAST and observe that EAST provides consistent improvements across all configurations tested. This demonstrates its versatility and complementary benefits to specialized extreme sparsity methods.

4.2. ImageNet

Prior methods like SynFlow and DCTpS were evaluated primarily on smaller datasets like CIFAR and Tiny-ImageNet. We extend these baselines to ImageNet through implementation and adaptation of their published code and evaluate the scalability of EAST on ImageNet using ResNet50 at sparsity 99.5% and 99.9%. Given the much shortened training epochs for ImageNet, we implement only the DyReLU phasing and weight sharing components, excluding cyclic sparsity. As presented in Table 2, EAST has demonstrated capability in maintaining network robustness on large-scale dataset, outperforming previous SOTA by a significant margin, achieving approximately 2% and 2.7% higher top-1 accuracy than RigL. This advantage is more notable when comparing to other methods including SynFlow and SET, which fail to maintain meaningful performance and collapse to random accuracy.

Method	Top-1 Acc (%)	Top-5 Acc (%)	Top-1 Acc (%)	Top-5 Acc (%)	Throughput (imgs/sec)	Latency (ms)
	Sparsity 99.50%		Sparsity 99.90%		Inference	
SynFlow	0.10	0.50	0.10	0.50	–	–
SET	0.10	0.50	0.10	0.50	–	–
RigL	32.50	58.58	8.53	24.18	–	–
DCT	0.10	0.50	0.10	0.50	–	–
DCT+RigL	19.99	43.34	6.62	18.84	1229.25	10.18
EAST (<i>ours</i>)	34.45	62.44	11.23	29.47	1638.41	6.80

Table 2. Performance comparison on ImageNet at extreme sparsity levels using ResNet50. For throughput and latency measurements, we use batch sizes of 2 and run 100 times and report the average.

Interestingly, we observe different dynamics on ImageNet compared to CIFAR experiments. While DCTpS showed competitive advantages on smaller datasets, it does not exhibit the same competitive advantages as seen before, even with the extra overhead. DCTpS alone results in performance collapse and it performs worse than RigL. When combined with RigL, the accuracy improvements are modest and may be attributed primarily to RigL’s robust dynamic sparse exploration policy, rather than the DCT offset. On the inference efficiency front, EAST demonstrates practical advantages. Unlike DCTpS, which relies on a dense DCT matrix, the model resulted from EAST does not have such drawback, as all DyReLU activations have been replaced with regular ReLU and thus runs just like the original ResNet model with ReLU. Our inference measurements show 1.5X lower latency and 1.33X higher throughput compared to DCTpS, while simultaneously achieving better accuracy. These results demonstrate that EAST can scale up to large datasets while maintaining computational efficiency and accuracy advantages over existing methods.

4.3. Ablation studies

4.3.1. Isolating DyReLU and Weight Sharing.

We first augment the standard RigL pipeline with only DyReLU phasing, replacing standard ReLU with DyReLU at initialization and gradually transitioning back to ReLU before the first learning rate schedule update. Weight sharing and cyclic sparsity are excluded in this isolated experiment. The results, summarized in Table 3 demonstrate a clear performance boost when utilizing DyReLU phasing, particularly at higher sparsity levels. At 99.99%, RigL completely loses its expressive capacity. However, as soon as DyReLU Phasing is used as a drop-in replacement for ReLU, it immediately starts converging. We observe that not only is training improved while DyReLU is in effect, but the performance continues to improve even after DyReLU has been completely phased out.

Improving gradient flow during early training has been shown to be critical for successfully training sparse net-

Model	Method	99.95% Sparsity	99.99% Sparsity
ResNet34	RigL w/ ReLU	81.47	10.03
	RigL w/ DyReLU	81.80	54.58
	RigL w/ WS	81.96	62.94
ResNet50	RigL w/ ReLU	30.14	10.00
	RigL w/ DyReLU	69.57	53.32
	RigL w/ WS	82.02	62.71

Table 3. Ablating DyReLU phasing on DST with evaluation at different sparsities. All settings are kept the same except the use of DyReLU phasing vs standard ReLU. Experiments were run on CIFAR-10. Results show improved performance with DyReLU Phasing, especially at higher sparsity levels.

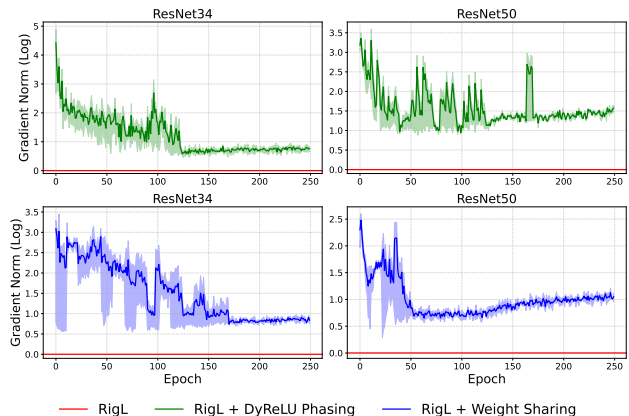


Figure 4. Gradient flow analysis. The top row compares gradient with and without DyReLU. The bottom row compares gradient with and without weight sharing.

works. Evci et al. [5] demonstrated that methods with better gradient flow, particularly during initialization and early training, consistently achieved superior performance. Building on this insight, we investigated the effect of DyReLU phasing on gradient flow in addition to measuring accuracy.

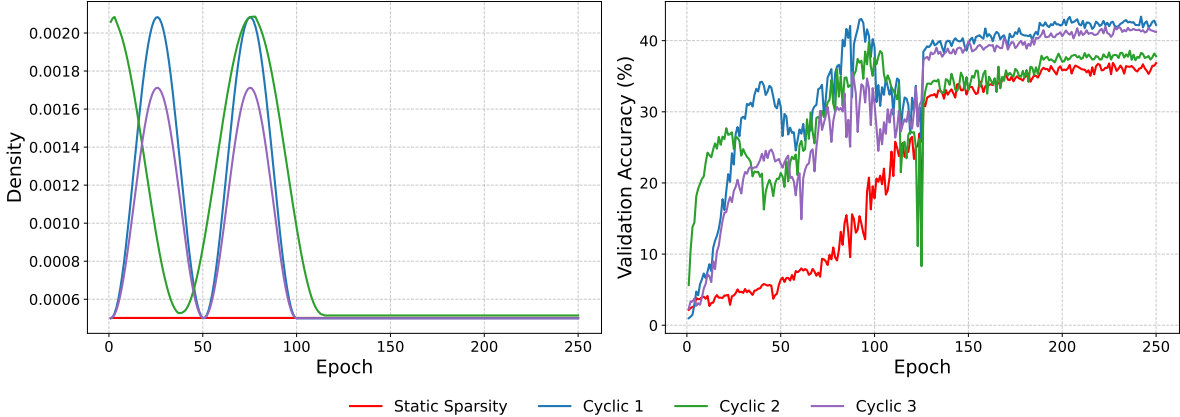


Figure 5. Ablation study using CIFAR-100 and ResNet34. Impact of cyclic sparsity on density (left) and validation accuracy (right) compared to static sparsity. All runs are performed using the same settings except cyclic sparsity schedule.

To analyze this, we computed the sum of the gradient norm of all layers, and compared the gradient flow during training between models using DyReLU phasing against those with standard ReLU. As shown in the top row of Figure 4, models using only standard ReLU have zero gradient norms at 99.99% sparsity and this is reflected in their collapsed accuracy. On the other hand, the networks with DyReLU phasing receive high gradient flow in the beginning where $\beta = 1$, during phasing where $0 < \beta < 1$, and maintains healthy gradient flow when $\beta = 0$. Results suggest that the network retains some of the gradient-boosting benefits initially provided by DyReLU. We conjecture that this is because DyReLU amplifies important features in the beginning and helps the network settle into a configuration that preserves gradients even after switching to standard ReLU. Gradient flow especially during early stages is a strong indicator of the DST’s success, and helps explain the performance gap between the methods. This supports our theoretical findings in the theorem, confirming that DyReLU phasing indeed provides greater gradient flow than the standard ReLU.

Similarly, we isolate the effect of weight sharing by adding only this mechanism to the RigL pipeline, keeping all other settings the same. Once again, gradient flow has been restored and we see a dramatic increase in gradient flow, as shown in the bottom row of Figure 4. This supports our hypothesis that creating additional gradient paths through weight sharing can help maintain stable training at extreme sparsities.

4.3.2. Effect of Cyclic Sparsity

Cyclic sparsity provides a flexible framework that allows networks to explore a wider parameter space. We perform an ablation study on the effect of cyclic sparsities using ResNet34 and CIFAR100 with a target sparsity of 99.95%. As shown in Figure 5, different cyclic schedules - whether

starting from high sparsity and decreasing, or from low sparsity and increasing, consistently outperform the static sparsity across all configurations. While each schedule can be tuned differently (e.g., altitude, length of cycle, etc.), we consistently observe improved parameter exploration and generalization.

We conclude that having some form of cyclic sparsity improves performance over static sparsity. However, the large number of possible configurations make systematic experimentation challenging. Future work will focus on tuning these schedules to identify optimal schedule for different datasets and architectures.

5. Conclusion

In this paper, we have presented EAST, a new DST approach with a strong focus on extreme sparsities that incorporates DyReLU phasing, weight sharing, and cyclic sparsity scheduling. Through extensive empirical evaluation on CIFAR-10, CIFAR-100 and ImageNet using ResNet-34 and ResNet-50, we demonstrated EAST’s ability to achieve competitive performance at extreme sparsities, surpassing existing methods. Each component of EAST individually contributes to maintaining robust gradient flow and optimizing parameter exploration at extreme sparsity, while their combined effect can further enhance performance stability. Our results highlight the potential in practical applicability in resource-constrained environments, establishing it as a scalable and effective method for highly compressed networks. This work paves the way for future research to consider and further optimize models at extreme sparsities, an area that previous studies have often overlooked or deemed infeasible.

Acknowledgments: Our work was supported by UK EPSRC (EP/V042270/1), a University PhD studentship, and HPC Maxwell.

References

- [1] Yinpeng Chen, Xiyang Dai, Mengchen Liu, Dongdong Chen, Lu Yuan, and Zicheng Liu. Dynamic relu. In *European conference on computer vision*, pages 351–367. Springer, 2020. 3, 12
- [2] Pau De Jorge, Amartya Sanyal, Harkirat S Behl, Philip HS Torr, Gregory Rogez, and Puneet K Dokania. Progressive skeletonization: Trimming more fat from a network at initialization. *arXiv preprint arXiv:2006.09081*, 2020. 1, 3
- [3] Tim Dettmers and Luke Zettlemoyer. Sparse networks from scratch: Faster training without losing performance, 2019. 1, 2
- [4] Utku Evci, Trevor Gale, Jacob Menick, Pablo Samuel Castro, and Erich Elsen. Rigging the lottery: Making all tickets winners, 2021. 1, 2, 5, 6, 11
- [5] Utku Evci, Yani Ioannou, Cem Keskin, and Yann Dauphin. Gradient flow in sparse neural networks and how lottery tickets win. In *Proceedings of the AAAI conference on artificial intelligence*, pages 6577–6586, 2022. 7
- [6] Jonathan Frankle and Michael Carbin. The lottery ticket hypothesis: Finding sparse, trainable neural networks. *arXiv preprint arXiv:1803.03635*, 2018. 1
- [7] Jonathan Frankle, Gintare Karolina Dziugaite, Daniel Roy, and Michael Carbin. Linear mode connectivity and the lottery ticket hypothesis. In *International Conference on Machine Learning*, pages 3259–3269. PMLR, 2020. 1
- [8] Jonathan Frankle, Gintare Karolina Dziugaite, Daniel M Roy, and Michael Carbin. Pruning neural networks at initialization: Why are we missing the mark? *arXiv preprint arXiv:2009.08576*, 2020. 3
- [9] Song Han, Huizi Mao, and William J Dally. Deep compression: Compressing deep neural networks with pruning, trained quantization and huffman coding. *arXiv preprint arXiv:1510.00149*, 2015. 1
- [10] Song Han, Jeff Pool, John Tran, and William Dally. Learning both weights and connections for efficient neural networks. In *Advances in neural information processing systems*, pages 1135–1143, 2015. 1
- [11] Kaiming He, Xiangyu Zhang, Shaoqing Ren, and Jian Sun. Delving deep into rectifiers: Surpassing human-level performance on imagenet classification. In *Proceedings of the IEEE international conference on computer vision*, pages 1026–1034, 2015. 3
- [12] Kaiming He, Xiangyu Zhang, Shaoqing Ren, and Jian Sun. Deep residual learning for image recognition. In *Proceedings of the IEEE conference on computer vision and pattern recognition*, pages 770–778, 2016. 5
- [13] Siddhant Jayakumar, Razvan Pascanu, Jack Rae, Simon Osindero, and Erich Elsen. Top-kast: Top-k always sparse training. *Advances in Neural Information Processing Systems*, 33:20744–20754, 2020. 3
- [14] Jie Ji, Gen Li, Lu Yin, Minghai Qin, Geng Yuan, Linke Guo, Shiwei Liu, and Xiaolong Ma. Advancing dynamic sparse training by exploring optimization opportunities. In *Forty-first International Conference on Machine Learning*, 2024. 3
- [15] Aditya Kusupati, Vivek Ramanujan, Raghav Somani, Mitchell Wortsman, Prateek Jain, Sham Kakade, and Ali Farhadi. Soft threshold weight reparameterization for learnable sparsity. In *International Conference on Machine Learning*, pages 5544–5555. PMLR, 2020. 1
- [16] Yann LeCun, John S Denker, and Sara A Solla. Optimal brain damage. In *Advances in neural information processing systems*, pages 598–605, 1990. 1
- [17] Namhoon Lee, Thalaisyasingam Ajanthan, and Philip HS Torr. Snip: Single-shot network pruning based on connection sensitivity. In *International Conference on Learning Representations*, 2019. 1, 3
- [18] Gen Li, Lu Yin, Jie Ji, Wei Niu, Minghai Qin, Bin Ren, Linke Guo, Shiwei Liu, and Xiaolong Ma. Neurrev: Train better sparse neural network practically via neuron revitalization. In *The Twelfth International Conference on Learning Representations*, 2024. 3
- [19] Hao Li, Asim Kadav, Igor Durdanovic, Hanan Samet, and Hans Peter Graf. Pruning filters for efficient convnets. In *International Conference on Learning Representations*, 2016. 1
- [20] Shiwei Liu, Tianlong Chen, Xiaohan Chen, Zahra Atashgahi, Lu Yin, Huanyu Kou, Li Shen, Mykola Pechenizkiy, Zhangyang Wang, and Decebal Constantin Mocanu. Sparse training via boosting pruning plasticity with neuroregeneration. *Advances in Neural Information Processing Systems*, 34:9908–9922, 2021. 2
- [21] Shiwei Liu, Lu Yin, Decebal Constantin Mocanu, and Mykola Pechenizkiy. Do we actually need dense over-parameterization? in-time over-parameterization in sparse training. In *International Conference on Machine Learning*, pages 6989–7000. PMLR, 2021. 3, 5
- [22] Zhuang Liu, Jianguo Li, Zhiqiang Shen, Gao Huang, Shoumeng Yan, and Changshui Zhang. Learning efficient convolutional networks through network slimming. In *Proceedings of the IEEE International Conference on Computer Vision*, pages 2736–2744, 2017. 1
- [23] Eran Malach, Gilad Yehudai, Shai Shalev-Schwartz, and Ohad Shamir. Proving the lottery ticket hypothesis: Pruning is all you need. In *International Conference on Machine Learning*, pages 6682–6691. PMLR, 2020. 1
- [24] Diganta Misra. Mish: A self regularized non-monotonic activation function. *arXiv preprint arXiv:1908.08681*, 2019. 3
- [25] Decebal Constantin Mocanu, Elena Mocanu, Peter Stone, Phuong H Nguyen, Madeleine Gibescu, and Antonio Liotta. Scalable training of artificial neural networks with adaptive sparse connectivity inspired by network science. *Nature communications*, 9(1):2383, 2018. 1, 2, 5
- [26] Hesham Mostafa and Xin Wang. Parameter efficient training of deep convolutional neural networks by dynamic sparse reparameterization. In *International Conference on Machine Learning*, pages 4646–4655. PMLR, 2019. 6
- [27] Vinod Nair and Geoffrey E Hinton. Rectified linear units improve restricted boltzmann machines. In *Proceedings of the 27th international conference on machine learning (ICML-10)*, pages 807–814, 2010. 3

- [28] Ilan Price and Jared Tanner. Dense for the price of sparse: Improved performance of sparsely initialized networks via a subspace offset. In *International Conference on Machine Learning*, pages 8620–8629. PMLR, 2021. [1](#), [3](#), [5](#)
- [29] Prajit Ramachandran, Barret Zoph, and Quoc V Le. Searching for activation functions. *arXiv preprint arXiv:1710.05941*, 2017. [3](#)
- [30] Hidenori Tanaka, Daniel Kunin, Daniel L Yamins, and Surya Ganguli. Pruning neural networks without any data by iteratively conserving synaptic flow. In *Advances in Neural Information Processing Systems*, pages 6377–6389. Curran Associates, Inc., 2020. [1](#)
- [31] Hidenori Tanaka, Daniel Kunin, Daniel L Yamins, and Surya Ganguli. Pruning neural networks without any data by iteratively conserving synaptic flow. *Advances in neural information processing systems*, 33:6377–6389, 2020. [1](#), [3](#), [5](#)
- [32] Stijn Verdenius, Maarten Stol, and Patrick Forré. Pruning via iterative ranking of sensitivity statistics. *arXiv preprint arXiv:2006.00896*, 2020. [3](#)
- [33] Chaoqi Wang, Guodong Zhang, and Roger Grosse. Picking winning tickets before training by preserving gradient flow. *arXiv preprint arXiv:2002.07376*, 2020. [1](#), [3](#)
- [34] Lu Yin, Vlado Menkovski, Meng Fang, Tianjin Huang, Yulong Pei, and Mykola Pechenizkiy. Superposing many tickets into one: A performance booster for sparse neural network training. In *Uncertainty in Artificial Intelligence*, pages 2267–2277. PMLR, 2022. [1](#), [3](#)
- [35] Lu Yin, Gen Li, Meng Fang, Li Shen, Tianjin Huang, Zhangyang Wang, Vlado Menkovski, Xiaolong Ma, Mykola Pechenizkiy, Shiwei Liu, et al. Dynamic sparsity is channel-level sparsity learner. *Advances in Neural Information Processing Systems*, 36, 2024. [3](#)
- [36] Geng Yuan, Xiaolong Ma, Wei Niu, Zhengang Li, Zhenglun Kong, Ning Liu, Yifan Gong, Zheng Zhan, Chaoyang He, Qing Jin, et al. Mest: Accurate and fast memory-economic sparse training framework on the edge. *Advances in Neural Information Processing Systems*, 34:20838–20850, 2021. [3](#)

Preliminaries

A.1 Dynamic Sparse Training

Let $\theta \in \mathbb{R}^N$ represent the set of all network weights, and let $\mathcal{M} \in \{0, 1\}^N$ be a binary mask that defines the active connections in the sparse model:

$$\theta_{\mathcal{M}} = \theta \circ \mathcal{M}$$

where \circ denotes element-wise multiplication. The sparsity s of the network is the fraction of pruned weights, defined as:

$$s = 1 - \frac{\|\mathcal{M}\|_0}{\|\theta\|_0}$$

where $\|\mathcal{M}\|_0$ is the number of active (non-zero) weights in the mask \mathcal{M} and $\|\theta\|_0$ is the total number of weights in a dense network. We follow the same criteria for updating connections used in RigL [4]. First, we prune by magnitude, where the smallest magnitude weights are pruned. When pruning, the top-K operation selects the weights with the smallest absolute values:

$$\mathcal{M}_{\text{prune}} = \text{ArgTopK}(-|\theta_{\mathcal{M}}|, (1 - s)\|\theta\|_0)$$

where s is the sparsity level and $\mathcal{M}_{\text{prune}}$ is the mask for pruned weights. We also adopt the gradient-based growth mechanism from RigL for regrowing weights, where the pruned weights with the largest gradients are reintroduced:

$$\mathcal{M}_{\text{grow}} = \text{ArgTopK}(|\nabla_{\theta} L|, s\|\theta\|_0)$$

where $\nabla_{\theta} L$ denotes the gradient of the loss function with respect to the weights. This ensures that important connections, as indicated by their gradients, are restored during training.

A.2 Dynamic ReLU

The DyReLU activation introduces adaptive piecewise linear activation functions that adjust to the input. Given input tensor $x = \{x_c\}_{c=1}^C$, where C is the number of channels, it is defined as:

$$y_c = f_{\theta(x)}(x_c) = \max_{1 \leq k \leq K} \{a_k^c(x)x_c + b_k^c(x)\}$$

where K is the number of functions, and k is the index. $a_k^c(x)$ and $b_k^c(x)$ are dynamically generated by a hyper-function $\theta(x)$ based on the input x . These dynamic coefficients allow DyReLU to provide more flexibility during training, and in our case enable better parameter exploration.

B. Proof

Here we provide the proof for the theorem in Section 3.1, which states that during the DyReLU to ReLU transition, the gradient flow is greater than the standard ReLU. We consider the two scenarios - before DyReLU phasing and during DyReLU phasing,

Before DyReLU phasing ($\beta = 1$), we can express the network as $f(x; \beta(0)) = f_{\text{DyReLU}}(x)$. Given the definition of DyReLU in A.2, the gradient using DyReLU can be expressed as:

$$\frac{\partial y_c}{\partial x} = \frac{\partial(a_k^c(x)x_c + b_k^c(x))}{\partial x} \quad (1)$$

Applying product rule to $a_k^c(x)x_c$ and chain rule:

$$a_k^c(x)x_c = a_k^c \frac{\partial x_c}{\partial x} + x_c \frac{\partial a_k^c}{\partial x} \quad (2)$$

$$\frac{\partial y_c}{\partial x} = a_k^c(x) \frac{\partial x_c}{\partial x} + x_c \frac{\partial a_k^c(x)}{\partial x} + \frac{\partial b_k^c(x)}{\partial x} \quad (3)$$

In DyReLU-B, a_k^c and b_k^c are negligible, $\frac{\partial a_k^c(x)}{\partial x} = 0$ and $\frac{\partial b_k^c(x)}{\partial x} = 0$. Therefore:

$$\frac{\partial y_c}{\partial x} = a_k^c(x) \frac{\partial x_c}{\partial x} = a_k^c(x) \quad (4)$$

For comparison, we express the gradients of both ReLU and DyReLU. The ReLU gradient is:

$$\frac{\partial \text{ReLU}(x_c)}{\partial x_c} = \begin{cases} 1 & \text{if } x_c > 0, \\ 0 & \text{if } x_c \leq 0 \end{cases} \quad (5)$$

Case 1: $x > 0$. We first establish the gradient norm equations for ReLU and DyReLU as follows:

$$\|\nabla \text{ReLU}(x)\| = \sqrt{\sum_{x^c > 0} 1^2} \quad (6)$$

$$\|\nabla \text{DyReLU}(x)\| = \sqrt{\sum_{x^c > 0} (a_k^c)^2} \quad (7)$$

Since a_k^c can be greater, equal to or less than 1, we rely on statistical evidence more than half are positive with a slope greater than 1 or negative [1], as well as our observation from Figure 4. Therefore, in a significant number of cases $a_k^c > 1$, and DyReLU provides a greater gradient than the standard ReLU. Since $\sqrt{\sum_{x^c > 0} (a_k^c)^2} > \sqrt{\sum_{x^c > 0} 1^2}$, we have $\|\nabla \text{DyReLU}(x)\| > \|\nabla \text{ReLU}(x)\|$.

Case 2: $x \leq 0$. While $\|\nabla \text{ReLU}(x)\| = 0$, DyReLU provides non-zero gradients through non-zero slopes a_k^c . When computing the gradient norm following Equation 7, since slopes a_k^c can be non-zero for negative inputs (as observed empirically in the paper), and $(a_k^c)^2 > 0$ for any non-zero slope regardless of the sign, we have $\|\nabla \text{DyReLU}(x)\| > 0 = \|\nabla \text{ReLU}(x)\|$.

During DyReLU phasing ($\beta \in (0, 1)$), we have:

$$f(x; \beta(t)) = \beta(t)f_{\text{DyReLU}}(x) + (1 - \beta(t))f_{\text{ReLU}}(x) \quad (8)$$

The gradient at any point during transition is:

$$\begin{aligned} \|\nabla f(x; \beta)\| &= \|\beta \nabla \text{DyReLU}(x) + (1 - \beta) \nabla \text{ReLU}(x)\| \\ &= \beta \|\nabla \text{DyReLU}(x)\| + (1 - \beta) \|\nabla \text{ReLU}(x)\| \\ &= \beta (\|\nabla \text{DyReLU}(x)\| - \|\nabla \text{ReLU}(x)\|) + \|\nabla \text{ReLU}(x)\| \\ &> \|\nabla \text{ReLU}(x)\| \end{aligned} \quad (9)$$

C. Implementation Details

We share the hyperparameters used from Section 4.1 and 4.2 in Table C.1.

Model	Method	Data	BS	Epochs	LR	LR Drop Epochs	Opt	WD	Init	Cyclic				ΔT_{dst}
										n	l	m	ΔT_{cs}	
ResNet-34	EAST	CIFAR-10/100	128	250	0.1	10x[75,150]	SGD(0.9)	1.0e-4	ERK	2	50	3	350	4000
ResNet-50	DCT+RigL+EAST	CIFAR-10/100	128	200	0.001	-	Adam	5.0e-4	ERK	2	50	3	100	100
ResNet-50	EAST	ImageNet	128	100	0.1	10x[25,50]	SGD(0.9)	1.0e-4	ERK	-	-	-	-	4000

Table C.1. Experiment hyperparameters used in this paper. Batch Size (BS), Learning Rate (LR), Epochs, Learning Rate Drop (LR Drop), Optimizer with Momentum (Opt), Weight Decay (WD), Sparse Initialization (Init), Cyclic Sparsity-Related hyperparameters - Number of Cycles (n), Length of Cycle (l), Maximum Parameter Multiplier (m), Update Frequency during Cyclic Sparsity (ΔT_{cs}), and Update Frequency for regular DST (ΔT_{dst}).